Field performance of concrete repair systems on a highway bridge structure

Cusson, D.; Qian, S. Y.; Hoogeveen, T. J.

Publisher's version / Version de l'éditeur:

ACI Materials Journal, 103, 5, pp. 366-373, 2006

Field performance of concrete repair systems on highway bridge

NRCC-47723

Cusson, D.; Qian, S.; Hoogeveen, T.

A version of this document is published in / Une version de ce document se trouve dans: ACI Materials Journal, v. 103, no. 5, Sept-Oct. 2006, pp. 366-373

FIELD PERFORMANCE OF CONCRETE REPAIR SYSTEMS ON A HIGHWAY BRIDGE

Daniel Cusson, Shiyuan Qian and Ted Hoogeveen

Biography: ACI member **Daniel Cusson** is a Research Officer at the National Research Council of Canada, Ottawa (Ontario) Canada, K1A 0R6. He is a member of ACI Committee 363 – High-Strength Concrete; member of RILEM TC 196 – Internal Curing of Concrete; and Adjunct Professor with University of Sherbrooke, Sherbrooke (Québec) Canada. His research interests include mechanical behavior of high-performance concrete structures at early ages, and field performance and durability assessment of rehabilitated concrete bridges.

ACI member **Shiyuan Qian** is a Senior Research Officer at the National Research Council of Canada. He is a member of ACI Committee 222 – Corrosion of Metals in Concrete. He is also member of The Electrochemical Society and NACE International. His research interests include corrosion assessment/protection of reinforced concrete structures, corrosion inhibition, metal dissolution/passivation and hydrogen permeation/embrittlement.

Ted Hoogeveen is a Technical Officer at the National Research Council of Canada. His expertise includes instrumentation and structural testing of reinforced concrete structures.

ABSTRACT

Six proprietary concrete repair systems were evaluated for their performance and durability under field conditions. The fieldwork consisted of repairing corrosion-damaged reinforced concrete barrier walls of a highway bridge, and installing embedded instrumentation for their continuous monitoring over three years. The results indicated that the proprietary repair systems reduced the

risk of corrosion in the patches; however, the risk of corrosion in the existing concrete was not reduced. All concrete repair systems suffered from shrinkage cracking.

Keywords: Concrete bridges; patch repairs; corrosion; durability; field performance; monitoring

INTRODUCTION

The cost of repairing and replacing deteriorated concrete bridges was estimated to be over $20 billion in the United States, and increasing at $500 million per year[1]. The main cause of this deterioration (e.g. cracking, delamination and spalling) is chloride-induced corrosion of the steel reinforcement. Corrosion prevention and repair of concrete bridge structures will continue to be a major concern for bridge owners for years to come.

Numerous laboratory studies[2,3,4] have been conducted to evaluate the performance of repair systems for concrete structures, however, discrepancies between laboratory performance results and actual field performance are frequently observed.[5,6] Satisfactory field performance is a key factor in the selection of concrete repair systems for the rehabilitation of corrosion-damaged concrete structures; however, the lack of representative data and practical guidelines makes the selection process difficult. Field investigations of repaired concrete structures are necessary to develop guidelines for (i) adequate selection of concrete repair systems, (ii) improved repair procedures, and (iii) extended durability of rehabilitated structures.[7,8]

The National Research Council (NRC) and the Ministry of Transportation of Ontario (MTO) established a research partnership in 1999 with five suppliers of concrete repair systems to evaluate the performance of these systems over three years under field conditions, including the

simultaneous effects of de-icing salt contamination, freeze-thaw cycles, and wet-dry cycles. The fieldwork consisted of repairing the 24-year old corrosion-damaged reinforced concrete barrier walls of a highway bridge near Renfrew (Ontario), using six different concrete repair systems, and installing embedded instrumentation in seven test sections for continuous monitoring. Key parameters such as temperature, relative humidity, corrosion potential, electrical resistance and mechanical strain were recorded twice daily at selected locations in the barrier wall. Laboratory tests were also conducted to characterize the concretes of the repair systems used in the field. This paper presents the performance evaluation results of different concrete repair systems installed on a bridge barrier wall monitored with embedded sensors over a three-year period.

RESEARCH SIGNIFICANCE

The performance of concrete repair systems for corrosion-damaged structures is often based on laboratory testing or visual field inspection. The former has a narrow focus, while the latter provides limited scientific understanding. The main objectives of this investigation are: (i) to evaluate the field performance of repaired concrete structures under simultaneous environmental effects; and (ii) to understand the factors governing the field performance of concrete repairs. The findings will enable structure owners to make well-informed decisions on material selection, the design, and execution of the repair work, and to provide manufacturers with relevant information for product improvement.

DESCRIPTION OF FIELD INVESTIGATION

Test structure

The structure selected for the study consisted of the barrier walls of a 2-lane, 3-span, 60-m [197 ft.] long concrete bridge, as illustrated in **Fig. 1**. The bridge is located on *Highway 17*, near

Renfrew (Ontario) Canada, and was built in 1975. The barrier walls were chosen for the application of the concrete repair systems because of their direct exposure to de-icing salts and their ease of access during repair and monitoring. The extent of concrete deterioration due to chloride contamination and the resulting reinforcement corrosion were representative of highway concrete structures exposed to typical environmental conditions in Ontario, Canada.

The barrier wall on each side of the deck consisted of ten 6-m [20 ft.] long sections separated by control joints. The barrier wall was 805 mm [32 in.] high, and had a thickness varying along the height from 250 mm [10 in.] at the top to 450 mm [18 in.] at the deck. Its reinforcement consisted of 20-mm [0.75 in.] uncoated black steel reinforcing bars, with 9 longitudinal bars in the cross-section and 200-mm [8 in.] spaced transverse reinforcement tied into the steel in the deck. The concrete cover to steel had an average thickness of 40 mm [1.6 in.], a standard deviation of 7 mm [0.28 in.] and a coefficient of variance of 16%, determined from 25 measurements on the barrier wall.[9] The repair work included the removal of deteriorated concrete and the appropriate surface preparation, as well as the application and curing of the concrete repair systems by their respective suppliers.

Concrete repair systems

Table 1 gives a generic description of the concrete repair systems investigated in this study, as well as the duration of wet curing provided in the field. The control repair system consisted of a conventional 30 MPa [4350 psi] Portland cement concrete, while the other systems were composed of proprietary repair concretes combined, in most cases, with protective rebar coatings and/or corrosion inhibitors. Due to confidentiality agreements between NRC and the manufacturers of the proprietary concrete repair systems, the commercial names of the products

used in this study cannot be revealed in the paper. Repair system No. 10 was the only system using a 50x50 mm [2x2 in.] galvanized steel wire mesh. The mesh was tied to the main reinforcement at a depth of 40 mm [1.6 in.] in the repair. This concrete repair system was applied without the use of forms and had no wet curing treatment. Repair systems Nos. 5 and 12 were identical in composition, and were installed in two separate test sections of the barrier wall.

A supporting laboratory testing program was conducted to determine some key properties of the concretes of the repair systems used in the field investigation. Throughout the duration of the repair work at the bridge (from Sept. 1999 to Nov. 1999), fresh concrete samples were taken on-site from each repair system for the following tests:

- Compressive strength on 100x200 mm [4x8 in.] cylinders, according to ASTM C39;
- Splitting tensile strength on 150x300 mm [6x12 in.] cylinders, according to ASTM C496;
- Freeze-thaw resistance on 75x75x250 mm [3x3x10 in.] prisms, according to ASTM C666;
- Water permeability on 100x50 mm [4x2 in.] disks, according to CRD C163.

The specimens were stored in an outdoor compound at the NRC in Ottawa to provide similar thermal conditions as for the test sections at the bridge in Renfrew. The samples were covered with layers of wet burlap and a layer of 12-mil plastic sheet to prevent moisture evaporation. Water was added to the burlap as required to prevent the concrete samples from drying over 28 days, which was the age of the concrete at testing. Note that concrete cores were not taken from the barrier walls, since no destructive testing was permitted on the bridge after rehabilitation.

Embedded instrumentation

Seven sections of the barrier wall on the South side of the bridge, with sufficient quantities of sound and delaminated concretes, were selected for monitoring. More than 100 sensors of various types were installed in seven large patches and the nearby old concrete, as well as in the ambient environment around the bridge. One of the concrete repair patches in each test section was selected for monitoring, and needed to be at least 800 mm [32 in.] long, 400 mm [16 in.] high, and 100 mm [4 in.] deep in order to accommodate the large array of sensors. Also, the instrumented patch had to be at least 800 mm [32 in.] away from the next patch in the same test section to enable the installation of sensors in the old concrete near the patch, and from the next test section to avoid undesired influences from different materials.

Since field studies require the consideration of several parameters that vary over the course of the investigation, many types of sensors were used to monitor the rapidly changing field conditions. As illustrated in **Fig. 2**, the sensors included: relative humidity and temperature sensors (RH), manganese dioxide (MnO_2) reference electrodes (RE), electrical resistance probes (RP), as well as strain gauges (SG) and strain-gauge devices (SD). For instance, in each test section, one RH sensor was inserted in the patch 50 mm [2 in.] from the surface (i.e. at the reinforcement level), and another RH sensor was inserted in a hole drilled in the substrate concrete 50 mm [2 in.] behind the 100-mm [4 in.] thick patch; four reference electrodes were installed in a row 10 mm [0.4 in.] behind one existing longitudinal reinforcing bar, which was located at a depth of 50 mm [2 in.] from the surface; strain gauges (SG), previously installed on a 800-mm long bar, were embedded longitudinally in the patch at a depth of 50 mm [2 in.] from the surface; and the strain-gauge device was positioned transversally in the patch near the patch/substrate interface. These

sensors were monitored twice daily over a 3-year period. The rationale for the selection and use of the sensors, as well as detailed information on their construction are given elsewhere.[10]

An automated data acquisition system was selected for the field study. As illustrated in **Fig. 3**, the data acquisition system consisted of four *Datataker DT505* data loggers from *Data Electronics Ltd* equipped with channel expansion modules and a cellular modem for remote communication with the host computer at NRC. The system was powered by three 12-volt lead-acid batteries, which were recharged by a set of three solar panels mounted on a 6 m [20 ft.] high pole (**Fig. 1**) because AC power was not available at the site. This system was selected for its capability to support various types of sensors, on-line data manipulation and statistical functions, and for its reliability as demonstrated in previous field projects.[6]

Calibration of instrumentation and correction of raw data

Relative humidity sensors - Measured values of relative humidity (RH) are affected by daily and seasonal temperature cycles. The effect of temperature on the measured RH was removed according to a procedure suggested by Pruckner and Gjorv.[11] As a result, the RH data presented in this paper were normalized for a temperature of 25°C.

Reference electrodes – The reference potential of MnO_2 electrodes is known to be stable in a constant environment. When embedded in hardening concrete, the change in the environmental conditions can cause their electrochemical potential to gradually reach a new equilibrium with the surrounding concrete. The embedded MnO_2 electrodes were calibrated by a standard copper/copper sulphate ($Cu/CuSO_4$) electrode at the beginning and at the end of the project in June 1999 and October 2002. The corrected half-cell potential data were obtained by adding the

corresponding calibration data (using linear interpolation) to the readings measured by the embedded electrodes.

Electrical resistance probes - The embedded probes installed in the patch and the nearby concrete measured electrical resistance in ohms (Ω). In order to obtain meaningful comparisons, the measured resistance values were converted into resistivity values (in kΩ-cm [kΩ-in.]) according to the following calibration procedure. Assuming that concrete is homogenous, the resistivity of concrete (ρ) was determined from the measured electrical resistance (R) using the relationship $\rho=RA/L$, where L is the distance between the two parallel pins of the probe (50 mm [2 in.]), and A is the equivalent cross sectional area of concrete where the current flows between the pins. The equivalent area is an unknown variable, which depends on the current distribution in the concrete due to changes in electrical resistivity. This unknown variable was determined by measuring the electrical resistance and resistivity of uniform materials (a solution containing high purity Millipore water and salt). The electrical resistance of the solution was varied by adding different amounts of salt to match the range of concrete resistances normally found in the field (from 10^3 to 10^6 ohms). The resistivity of a given solution in an electrochemical resistivity cell of known cross-sectional area (A) and distance (L) was determined with an LCR meter. The resistance of the same solution was then measured with a probe identical to those used at the bridge to determine A for a given resistance. For different solutions having a wide range of electrical resistances, the relationship between A and R was obtained.

Strain gauges - The strain data presented in this paper represent a change in the total strain from the first day of data acquisition (Nov. 19, 1999), which occurred a few weeks after installation of

the repair systems in the barrier wall (from Oct. 6 to Nov. 1, 1999). As a result, the measured strain did not include the early shrinkage strain that probably had occurred in the few weeks after repair. The total strain was calculated by adding the mechanical strain, which was measured by the strain gauges, to the thermal strain, which is the product of the measured concrete temperature change and the thermal expansion coefficient of the instrumented rebar. The stability of the strain readings was verified using dummy gauges left unstrained in the data logger enclosure. The results showed a negligible drift of only 10με after three years.

FIELD MONITORING RESULTS

Environmental conditions

Temperature has a significant effect on the corrosion process. It is known that a rise in temperature results in an increase of the rate of corrosion.[12] Moreover, the moisture level in concrete also influences reinforcement corrosion as it affects chloride penetration, electrical resistivity, and availability of oxygen. It is therefore important to know the prevailing environmental conditions for the analysis of the parameters that govern the performance of the concrete repair systems in the field, such as corrosion potential, electrical resistivity, strain, etc.

Between Nov. 1999 and Nov. 2002, the concrete temperature measured in the barrier wall displayed a seasonal pattern between –20°C [–5°F] and +30°C [85°F]. No significant temperature differences were observed between the different test sections at any given time or between the new and old concretes. Daily temperature fluctuations of up to 10°C [18°F] were recorded in the barrier wall. The concrete temperature data were also used to estimate the number of freeze/thaw (F/T) cycles that occurred in the concrete barrier wall during the three winters of the study.

Assuming that capillary water in conventional concrete freezes at about –5°C [23°F] and thaws at 0°C [32°F] (as suggested by Neville[13]), it was estimated that 7, 8, and 13 freeze/thaw cycles occurred annually in the barrier wall during the three winter periods, respectively. **Fig. 4** shows such data for the third winter. It is important to note, however, that the effect of uncontrolled freeze-thaw cycles observed in the field cannot be compared directly to the effect of controlled F/T cycles simulated in the laboratory according to ASTM C666, as there are significant differences in the range and rate of change in both temperature and moisture. It will be shown later that the freeze-thaw cycles, which occurred at the bridge during the three winters, were severe enough to cause freeze-thaw deterioration in the concrete patches of one test section.

Fig. 5 presents the monthly average of RH measured in the concrete patches, in which each curve corresponds to one repair system (see Table 1 for the system codes). The concrete RH decreased in all test sections from Nov. 1999 to Nov. 2002 due to gradual drying, combined with a typical seasonal fluctuation, as expected. Two trends were observed: (i) Sections 2, 3, 6, 10 and the control section displayed RH values decreasing from 90-100% to 85-90% three years later; and (ii) Sections 5 and 12 displayed lower RH values overall, decreasing from 85-90% to 75-80% during the same period. These trends were confirmed by the measurements of electrical resistivity, which will be discussed later. The low RH in the patches of Sections 5 and 12 may be the result of self-dessication in the concrete.

The RH was also measured in the substrate (behind the patch), as shown in **Fig. 6**. In general, the RH measured in the concrete substrate was similar to the RH measured in the patch (except Sections 5 and 12, in which the patches displayed lower RH values). Normally, in unrepaired old concrete, RH values would be expected to be lower than those shown in **Fig. 6** due to a long drying period. In this study, however, a different trend was observed in the old concrete near the

patches where high RH values were measured shortly after repair. It is believed that the old concrete substrate in contact with the newly-placed concrete patch absorbed moisture from the patch due to its relatively high permeability. After some time, equilibrium was reached between the patch and the nearby substrate, and a gradual drying took place simultaneously.

According to ACI Committee 222,[14] the risk of reinforcement corrosion can be considered low in dry concrete (RH < 50%) due to an impeded electrolytic process, or in fully saturated concrete due to low oxygen concentration. In partially saturated concrete, however, the risk of corrosion becomes higher since oxygen can easily diffuse through concrete down to the reinforcement, which will accelerate the corrosion process. As noted above, the RH values measured in the concrete patches and substrates were between 75% and 95% for the majority of the time. With the regular use of de-icing salts in winter, one can conclude that the environmental conditions at the bridge were favorable to reinforcement corrosion during the field investigation.

Reinforcement corrosion potential

When a concrete patch is installed on a chloride-contaminated concrete substrate, the reinforcement corrosion potential will become less negative in the patch due to its high initial alkalinity and the significant reduction in chloride content. As a result, the reinforcing steel in the patch will act as a cathode, and the steel in the old concrete, as an anode, causing macro-cell corrosion in the substrate near the patch. Therefore, the difference between the potential in the patch and that in the nearby old concrete represents the driving force for macro-cell corrosion. In this study, a set of four MnO_2 electrodes were installed in the patch and the nearby old concrete to provide a profile of corrosion potential along the length of an existing reinforcing bar (**Fig. 2**).

Fig. 7 shows the monthly average of the corrosion potential of the reinforcing steel vs. CSE measured in the patch on electrode RE4 (located 400 mm [16 in.] away from the old concrete). The values for the winter months are not shown because the readings were disturbed due to the frozen electrolyte in the concrete pores. As shown in **Fig. 7**, the corrosion potential in the control section shifted towards more negative values, from –320 mV in Nov. 1999 to –470 mV three years later, indicating a risk of reinforcement corrosion. In all other test sections, the corrosion potential in the patches remained practically unchanged with values between –200 mV and –350 mV, a range indicating that corrosion is uncertain according to ASTM C876. The higher risk of corrosion observed in the patch of the control section may be due to the lack of corrosion protection of the control repair system (e.g. no rebar coating, no corrosion inhibitor, etc.).

In **Fig. 7**, it can be observed that the initial values of the corrosion potential for the different concrete patches varied considerably between –250 mV and –350 mV. Corrosion was not expected at that time on the patch reinforcement because it was properly sandblasted and cleaned before the application of the concrete repair systems. This wide range of initial potential values may be the effect of different oxygen concentrations and different types of corrosion inhibitors used in the concrete repair systems, complicating the assessment of corrosion.[8] For example, dense concrete can lead to oxygen depletion at the steel-concrete interface, resulting in more negative readings of the corrosion potential. Moreover, an anodic corrosion inhibitor can shift the half-cell potential towards more positive values, while a cathodic inhibitor can produce the opposite shift in potential. Therefore, the change in corrosion potential over time is used in this study in order to assess the risk of corrosion of a given repair system.

Fig. 8 presents the monthly average of the corrosion potential of the reinforcing steel vs. CSE measured in the old concrete on electrode RE1 (located 400 mm [16 in.] away from the patch). The curves show that the corrosion potential of the old concrete in all test sections shifted towards more negative values by more than 100 mV during the three-year period. This is an indication that the risk of corrosion in the substrate was still increasing after the rehabilitation.

Concrete electrical resistivity

In general, the larger the electrical resistivity of the concrete, the smaller the corrosion rate of the reinforcement. **Fig. 9** presents the monthly average of electrical resistivity in the concrete patches. The values of electrical resistivity ranged from 10 kΩ-cm [4 kΩ-in.] to 10,000 kΩ-cm [4,000 kΩ-in.] depending on the environmental conditions and the test sections monitored. Considering that dry conventional concrete has a known electrical resistivity close to 1,000 kΩ-cm [400 kΩ-in.], values as high as 10,000 kΩ-cm [4,000 kΩ-in.] seem reasonable for high-density, low permeability concrete in dry conditions. The trends observed for the electrical resistivity are in agreement with the trends for the measured RH values (but inversely proportional). Due to continuous drying, an overall increase in electrical resistivity by almost an order of magnitude is observed from Nov. 1999 to Nov. 2002, corresponding to an overall decrease of approximately 10% in RH for the same period. The concrete patches in Section 2 and the control section had the lowest resistivity values overall (and highest RH values), while the patches of Sections 5 and 12 had the highest resistivity values overall (and lowest RH values). A wide seasonal variation of resistivity is also observed, with high resistivity corresponding to low RH and low temperature measured in the winter. This wide variation of resistivity is explained by the significant effect of temperature and RH on the electrical resistivity of concrete, especially during winter when the electrolyte in the concrete pores is frozen leading to very high values of

concrete resistivity. Typical values reported in the literature may not correspond to these high winter peaks since field surveys are usually not conducted under freezing temperatures.

Fig. 10 illustrates the monthly average of electrical resistivity of the old concrete. The values ranged from 1 kΩ-cm [0.4 kΩ-in.] to 100 kΩ-cm [40 kΩ-in.] depending on the salt content in the old concrete and the environmental conditions. As expected, the resistivity and its variation between different sections are smaller than for the concrete patches. The narrow range of values is explained by the fact that the old concrete in the different test sections had the same mix design. The low values may be due to the high porosity and high de-icing salt content of the old concrete, which was about 0.7% by mass of concrete,[9] measured near the surface in 1999.

Concrete cracking and delamination

Vertical transverse cracking was monitored by horizontal strain gauges installed on a longitudinal reinforcing bar embedded in the patch. As well, delamination of the repair was monitored by a short horizontal strain-gauge device embedded in the patch in the transverse direction (i.e. perpendicular to the main interface with the substrate).

Fig. 11 presents the monthly average of the total transverse strain (perpendicular to the face of the wall) in the concrete patches. The calculated thermal strain is also shown in the insert. The total strain measured transversally in the concrete patches clearly displays a pattern very similar to that of the thermal strain, confirming that the main component of the total strain in the long term was the thermal strain. Since no sudden changes in the total transverse strain were observed in the patches, it may be concluded that no delamination had formed in any of the instrumented patches between 1999 and 2002.

Fig. 12 presents the monthly average of the total longitudinal strain (along the length of the wall) in the concrete patches. Initially, the total strain measured longitudinally in the concrete patches clearly displayed a pattern similar to that of the thermal strain. However, after one year, sharp deviations from the normal seasonal trend were observed in many patches, indicating the onset of vertical shrinkage cracking in the control section in Dec. 2000, Section 12 in July 2001, Section 5 in Dec. 2001, Section 6 in April 2002, and Section 2 in August 2002. A careful examination of the repaired barrier wall sections in October 2003 revealed several vertical shrinkage cracks in the concrete patches of all test sections. **Fig. 13** presents a photograph of the concrete patch in Section 2, where vertical shrinkage cracks can be seen. This cracking pattern was observed typically in all concrete repair systems investigated in the study.

LABORATORY TESTING RESULTS

The results of the laboratory tests conducted on the concrete of each repair system are presented in **Table 2**. Each result is an average obtained from three test samples. Note that the field-cast samples for the laboratory tests had a standard wet curing period of 28 days, which is longer than the curing periods provided to concrete repair systems in the field (**Table 1**).

Compressive and tensile strengths

Except for the repair concrete No. 10, all repair concretes had strengths above the 28-day design strength of 30 MPa [4350 psi] specified by MTO for the repair work, with compressive strengths as high as 51 MPa [7395 psi] for the concretes Nos. 5 and 12. The repair concretes Nos. 5, 6 and 12 had high splitting tensile strengths (over 4.5 MPa [653 psi]), which is an advantage for the prevention of stress-induced cracking from restrained shrinkage or corrosion. Note that other

factors such as shrinkage, stiffness and creep of the concrete, as well as the degree of restraint in the structure are also important factors affecting the durability of a repair system.

Freeze-thaw resistance

According to ASTM C666, a concrete sample subjected to rapid freeze-thaw cycles is considered failed when axial expansion exceeds 0.1% prior to 300 cycles. All concretes, except concrete No. 2, passed the test with very small changes in average length. No significant loss in weight was measured. For concrete No. 2, the samples failed after 152 freeze-thaw cycles on average, showing large transverse cracks in the middle of the three concrete samples. A large axial expansion of 0.87 % was measured on average just before cracking. **Fig. 13** presents a photograph of the repair in Section 2 taken at the age of four years, in which freeze-thaw deterioration was observed.

Water permeability

The water permeability of the concrete of the repair systems was tested according to CRD C163. According to Neville,[13] a coefficient of permeability smaller than 1×10^{-11} m/s [3.3×10^{-11} ft./s] is representative of very low permeability; a value between 1×10^{-11} m/s [3.3×10^{-11} ft./s] and 1×10^{-10} m/s [3.3×10^{-10} ft./s] corresponds to moderate permeability, and a value greater than 1×10^{-10} m/s [3.3×10^{-10} ft./s] indicates a high permeability. Based on these criteria, concretes Nos. 2 and 10 had moderate and high coefficients of permeability, respectively, while the other repair concretes had very low water permeability.

OVERALL PERFORMANCE OF REPAIR SYSTEMS

The durability of a repaired concrete structure will ultimately depend on the ability of a repair system to perform under the simultaneous effects of many environmental and mechanical factors, which also interact with each other. In order to assess the overall performance of the concrete repair systems, multiple sets of corrosion-related measurements (**Table 3**) and mechanical/durability-related measurements (**Table 2)** were selected for the analysis.

Risk of reinforcement corrosion in the patch

The risk of corrosion in the patch was assessed by the change in corrosion potential from Nov. 1999 to Nov. 2002 (**Table 3**). A significant negative change can be viewed as a high corrosion risk in the patch. In addition, a high electrical resistivity of the patch will reduce the current density, which in turn will reduce the corrosion of steel in the patch. **Table 3** provides the electrical resistivity of the patch measured near the end of the project (Sept. 2002, which had a monthly average temperature of 20°C [68°F]).

From these results, it is found that the patches of the control section and Section 2 had the highest risks of corrosion, with the largest negative potential changes over 3 years and the lowest electrical resistivity values. On the other hand, all other repair systems provided satisfactory corrosion protection in the patch, with positive changes in potential over time and relatively high values of electrical resistivity. However, the premature shrinkage cracks observed in the patches of all repair systems will accelerate the ingress of moisture and chlorides to the reinforcement and will most likely increase the risk of corrosion in the patches of the repair systems in the future.

Risk of corrosion in the old concrete near the patch

The risk of corrosion in the old concrete near the patch due to macro-cell corrosion was assessed by the difference in corrosion potential between the old concrete and the patch at an age of three years in Sept. 2002 (**Table 3**). A large negative potential difference can be viewed as a high risk of macro-cell corrosion, but this risk can be reduced if the patch has a high electrical resistivity (**Table 3**). Moreover, the risk of micro-cell corrosion in the old concrete was also assessed by the change in corrosion potential in the old concrete from Nov. 1999 to Nov. 2002 (**Table 3**), where a significant negative change can be viewed as a high risk of corrosion.

These results show that the repair systems in the control section and Section 2 had the lowest risks of macro-cell corrosion in the old concrete near the patches. For the other systems, the risk of macro-cell corrosion is also considered low, since they all had very high values of electrical resistivity. On the other hand, all test sections had high negative changes in potential in the old concrete over time (which also had low electrical resistivity) indicating that the repair systems had little influence on the reinforcement corrosion (micro-cell) in the old concrete.

Expected durability in the field

The laboratory measurements indicated that the repair concretes Nos. 3, 5, 6 and 12 consistently performed very well with adequate strength, excellent freeze-thaw resistance and very low water permeability. A correlation between the laboratory and the field measurements of electrical resistivity and corrosion potential in the patches can be established. For instance, those repair systems, made of dense and strong concretes, had the highest resistivity values and the more stable corrosion potentials in the field. As a result, concrete repair systems made of such “high-performance” concretes may be effective in preventing micro-cell corrosion in the patch as well

as macro-cell corrosion in the old concrete near the patch (as shown in **Figs. 7-8** and **Table 3**). However, it was also demonstrated (in **Fig. 8** and **Table 3**) that all the repair systems investigated in this study had little influence on the micro-cell corrosion developing in the old concrete. Moreover, all repair systems failed to prevent shrinkage cracking in the patches, which may accelerate chloride ingress through the cracks and initiate localized corrosion in the near future.

SUMMARY AND CONCLUSIONS

Different concrete repair systems applied on the barrier walls of a highway bridge were subjected to harsh environmental and loading conditions. The analysis of the data obtained from 3 years of remote monitoring and laboratory tests yields the following conclusions:

1. Remote monitoring with embedded sensors in repair systems and old concrete provided an effective method for performance evaluation of repair systems on barrier walls.
2. The risks of micro-cell corrosion in the concrete patches were the lowest in the field for the repair concretes that had the highest strengths, the highest freeze-thaw resistances and the lowest values of permeability measured in the laboratory.
3. The risks of macro-cell corrosion (anodic ring effect) in the nearby old concrete were the lowest in the field for the repair concretes that had material properties similar to those of the old concrete, with lowest strengths and highest values of permeability.
4. The risk of micro-cell corrosion in the old concrete continued to increase after the rehabilitation, indicating that the concrete repair systems had little influence on the reinforcement corrosion developing in the old concrete.
5. Vertical shrinkage cracks were observed in the concrete patches of the repair systems tested in this study. As a result, reinforcement corrosion, due to chloride ingress in the concrete patches, may initiate in the near future.

ACKNOWLEDGMENTS

The authors acknowledge the close collaboration of the following project partners: MTO's Materials Engineering and Research Office; Roger Willoughby of NRC's Industrial Research Assistance Program; and Noel Mailvaganam of NRC's Institute for Research in Construction. The financial support from Axim-Italcementi Group, King Packaged Materials Company, Master Builders Technologies, Sika Canada, Silcrete Technologies and The Regional Municipality of Peel is also thankfully acknowledged.

REFERENCES

1. Smith, J.L., Virmani, Y.P., "Materials and Methods for Corrosion Control of Reinforced and Prestressed Concrete Structures in New Construction" *Report No. FHWA-RD-00-081*, FHWA, August 2000, 88 pp.

2. Emberson, N.K., Mays, G.C, "Significance of Property Mismatch in the Patch Repair of Structural Concrete Part 1: Properties of Repair Systems," *Magazine of Concrete Research*, V. 42, No. 152, 1990, pp. 147-160.

3. Yuan, Y.-S. and Marosszeky, M., "Major Factors Influencing the Performance of Structural Repair," ACI Special Publication SP-128-50, 1991, pp. 819-837.

4. Poston, R.W., Kesner, K, McDonald, J.E., Vaysburd, A.M., Emmons, P.H., "Concrete Repair Material Performance – Laboratory Study," ACI Materials Journal, Vol.98, No.2, March-April 2001, pp. 137-147.

5. Gulis, E.W., Lai, D., Tharambala, B, "Performance and Cost Effectiveness of Substructure Rehabilitation/Repair Strategies,"*Draft Report*, Ministry of Transportation of Ontario, Downsview, Canada, 1998.

6. Qian, S., Cusson, D., “Electrochemical Evaluation of the Performance of Corrosion-Inhibiting Systems in Concrete Bridges," *Cement and Concrete Composites*, Vol.26, No.3, April 2004, pp. 217-233.

7. Pines, D., Aktan, A.E., “Status of Structural Health Monitoring of Long-Span Bridges in the United States,” *Progress in Structural Engineering & Materials*, Sept. 2002, pp. 372-380.

8. Hansson, C. M., Seabrook, P.T., Marcotte, T.D, “In-Place Corrosion Monitoring,” *Concrete International*, July 2004, pp. 59-65.

9. Berszakiewicz, B., Pianca, F., Wojcik, C., Cusson, D., Qian, S., Hoogeveen, T., “Field Investigation of Proprietary Patching Systems for Concrete Repairs – A Joint MTO and NRC Report, Report No. MERO-012, Ministry of Transportation of Ontario, Downsview, Canada, Nov. 2004.9.

10. Cusson, D., Hoogeveen, T., Repette, W., Qian, S., Berszakiewicz, B., Pianca, F., Willoughby, R., Mailvaganam, N., “Remote Monitoring of Concrete Repairs on a Highway Bridge,” *28th Annual Conference of the CSCE*, London, Canada, 2000, 8 pp.

11. Pruckner, F., Gjorv, O.E, “Measurements of Relative Humidity in Concrete,” *3rd Int. Conf. on Concrete Under Severe Conditions*, Ed.: N. Banthia, K. Sakai & O.E. Gjorv, Vancouver, Canada, 2001, pp. 1489-1496.

12. Shiessl, P., Raupach, M, “Influence of Concrete Composition and Microclimate on the Critical Chloride Content in Concrete,” In: *Corrosion of Reinforcement in Concrete*, Ed.: C.L. Page, K.W.J. Treadaway, & P.B. Bamforth, Society of Chemical Industry, Elsevier Applied Science, London, England, 1990, pp. 49-58.

13. Neville, A.M. “Properties of concrete,” 4th ed., Longman Group Limited, Essex, England, 1996.

14. ACI Committee 222, “Protection of Metals in Concrete Against Corrosion,” American Concrete Institute, Farmington Hills, 2001, 41 pp.

TABLES AND FIGURES

List of Tables:

List of Figures:

Table 1 – Generic description of the investigated concrete repair systems

System Code	Generic Product Description	Duration of wet curing
Ctrl	- conventional repair concrete (control)	15 days
2	- silicate-based rebar coating - repair concrete - silicate-based concrete coating	2 days
3	- air-entrained self-compacting concrete	14 days
5, 12	- corrosion inhibitor on the reinforcement - repair concrete incl. anodic corrosion inhibitor - corrosion inhibitor at the concrete surface	5 days
6	- polymer-modified cementitious rebar coating - repair concrete incl. corrosion inhibitor - water-based curing compound	6 days
10	- epoxy resin-based cementitious anticorrosion rebar coating - galvanized steel wire mesh - fiber-reinforced sprayable repair mortar incl. corrosion inhibitor - penetrating corrosion inhibitor at the concrete surface	-

Table 2 – Laboratory test results obtained for the repair concretes

Laboratory Test	Concrete Code						
	Ctrl	**2**	**3**	**5**	**6**	**10**	**12**
Compressive strength, MPa [ksi]	31 [4.5]	36 [5.2]	46 [6.7]	51 [7.4]	46 [6.7]	25 [3.6]	51 [7.4]
Splitting tensile strength, MPa [ksi]	3.2 [0.46]	3.1 [0.45]	3.3 [0.48]	4.5 [0.65]	4.7 [0.68]	2.5 [0.36]	4.5 [0.65]
Freeze-thaw resistance, % length change	0.02	0.87	0.01	0.04	0.02	0.01	0.04
Water permeability, 10^{-12} m/s [ft./s]	2 [6.6]	62 [203]	≈ 0 [≈ 0]	≈ 0 [≈ 0]	≈ 0 [≈ 0]	170 [558]	≈ 0 [≈ 0]

Table 3 – Selected field test results obtained for the concrete repair systems

Field Test	System Code						
	Ctrl	**2**	**3**	**5**	**6**	**10**	**12**
Potential change in new concrete, mV (from Nov. 99 to Nov. 02)	-156	-72	27	110	19	71	139
Potential change in old concrete, mV (from Nov. 99 to Nov. 02)	-85	-148	-192	-133	-111	-120	-124
Potential diff. between old/new concretes, mV (in Sept. 02)	-18	-43	-142	-102	-125	-132	-102
Resistivity in new concrete, kΩ-cm [kΩ-in.] (in Sept. 02)	31 [12]	102 [40]	117 [46]	248 [98]	724 [285]	158 [62]	784 [309]
Resistivity in old concrete, kΩ-cm [kΩ-in.] (in Sept. 02)	4 [1.6]	7 [2.8]	4 [1.6]	2 [0.8]	29 [11]	7 [2.8]	38 [15]
Shrinkage cracks? (in Oct. 03)	Yes	Yes	Yes	Yes	Yes	Yes	Yes

Fig. 1 – Test bridge during repair and instrumentation

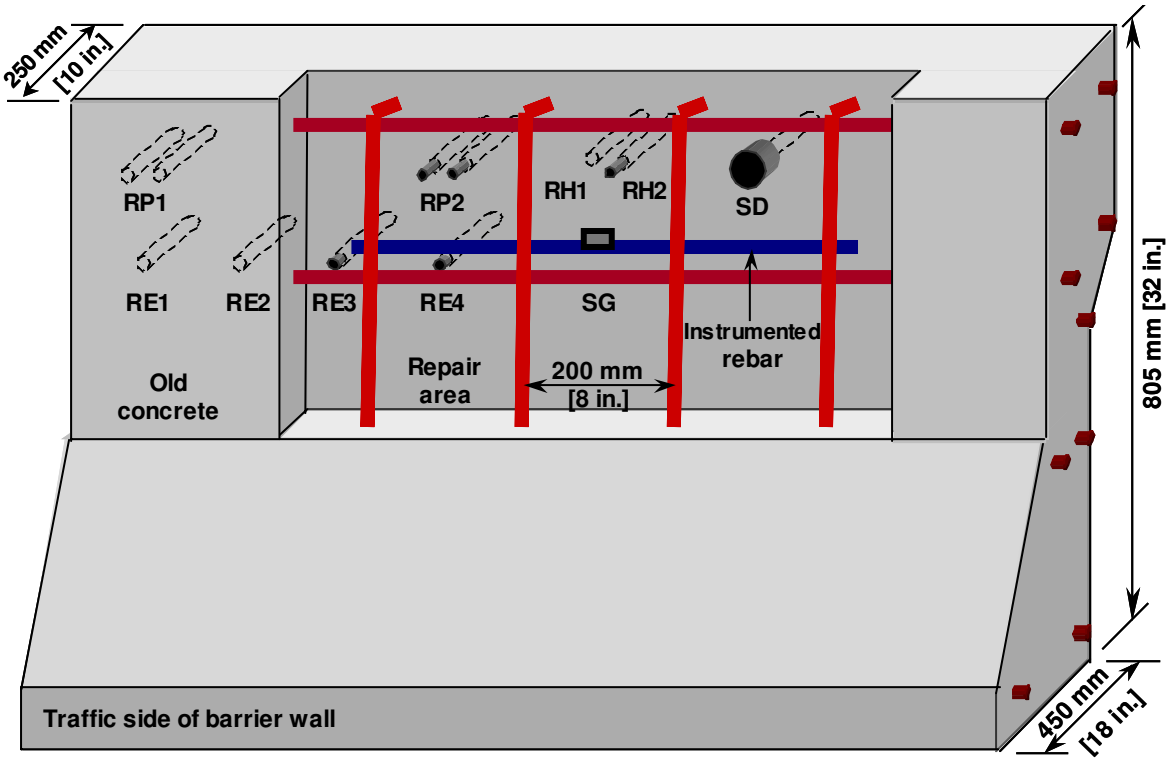

Fig. 2 – Location of sensors at the centre of a typical test section (total length of section: 6 m [20ft.])

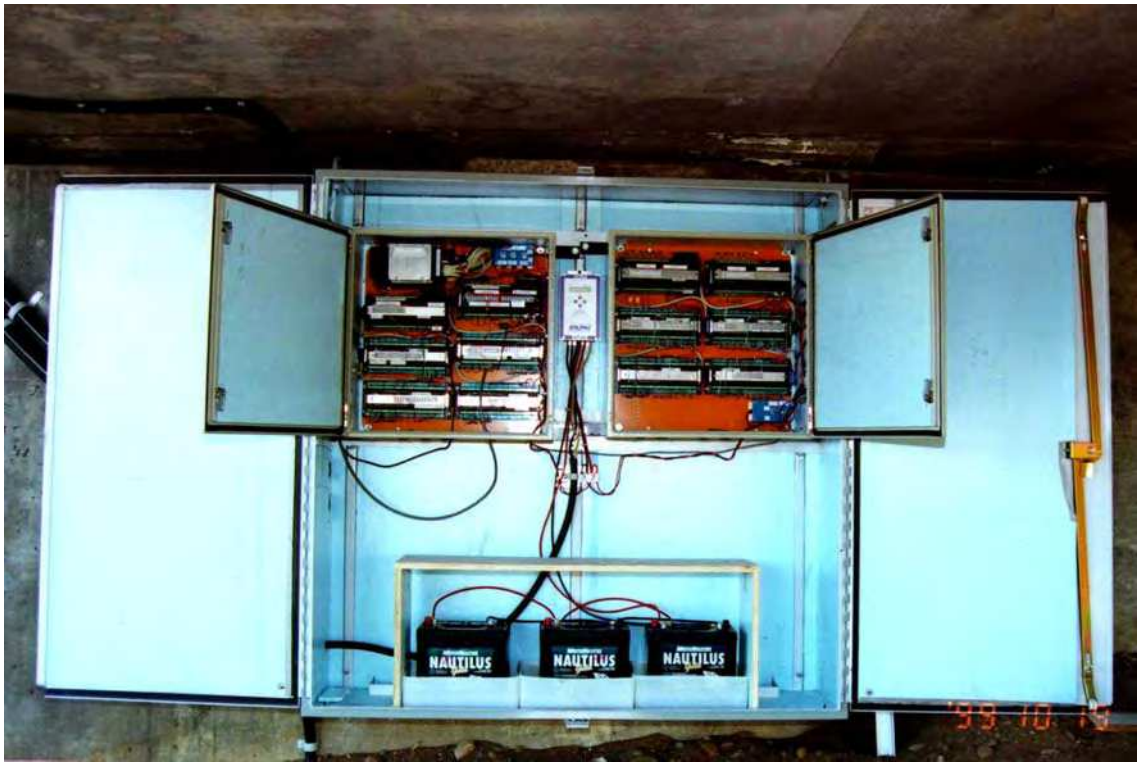

Fig. 3 – Data logging system installed underneath bridge deck

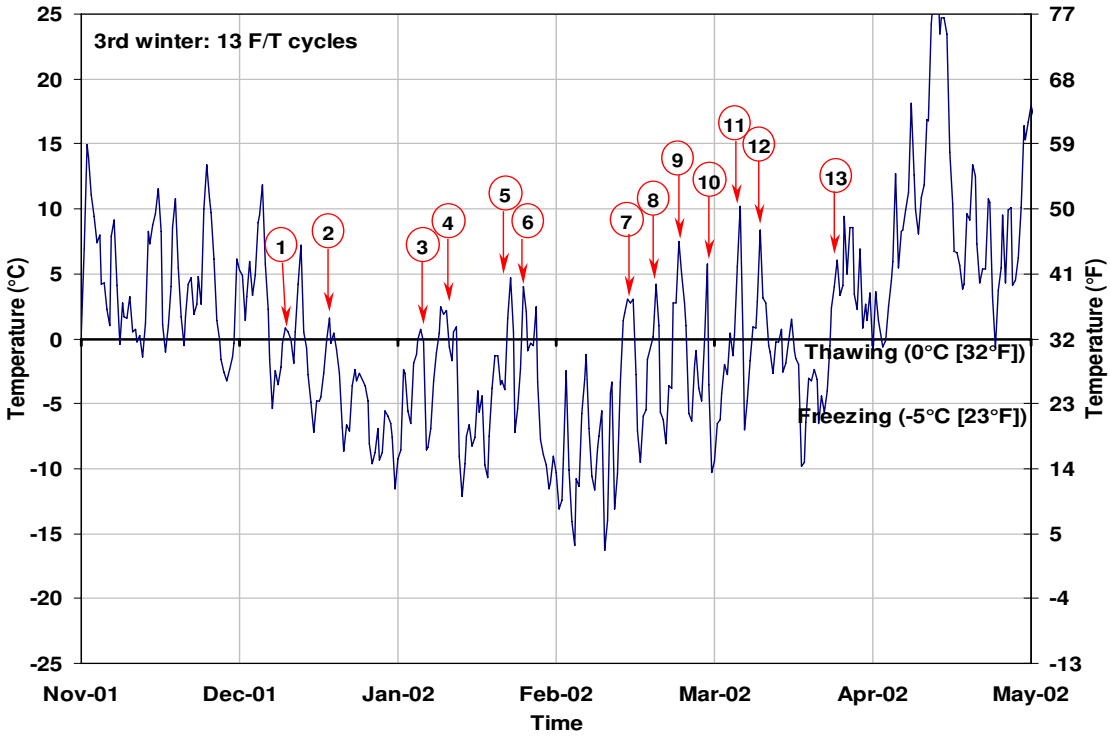

Fig. 4 – Concrete temperature and freeze-thaw cycles during winter 2001/2002

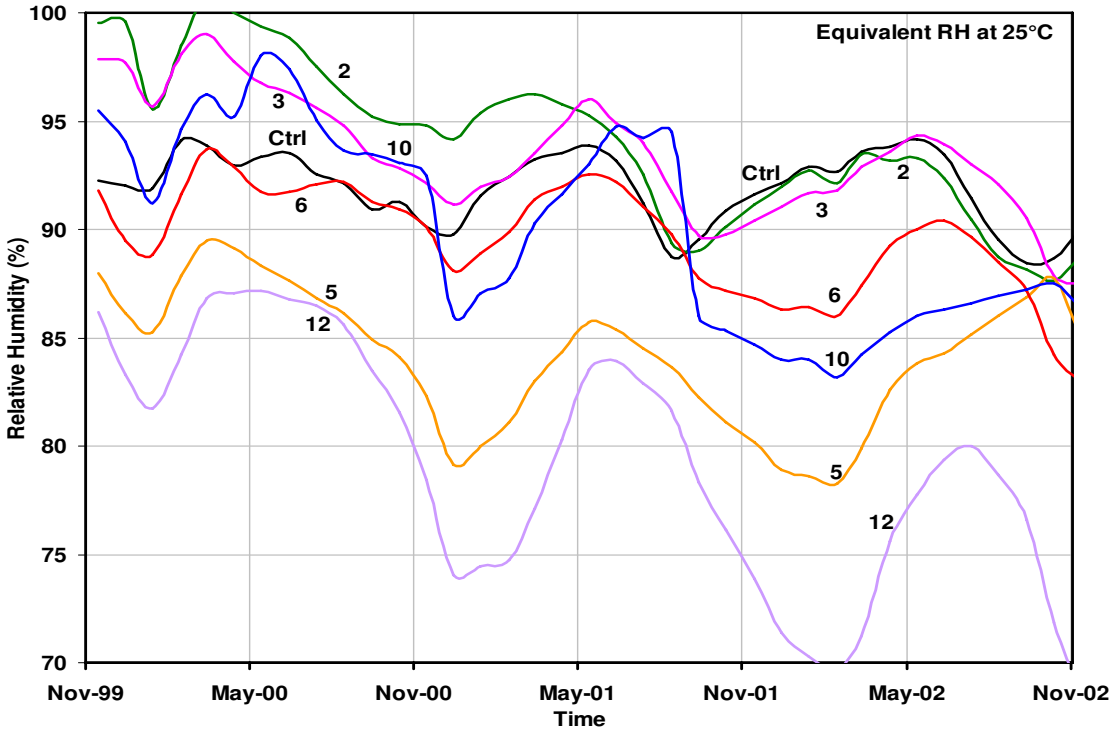

Fig. 5 – Monthly average relative humidity in concrete patches

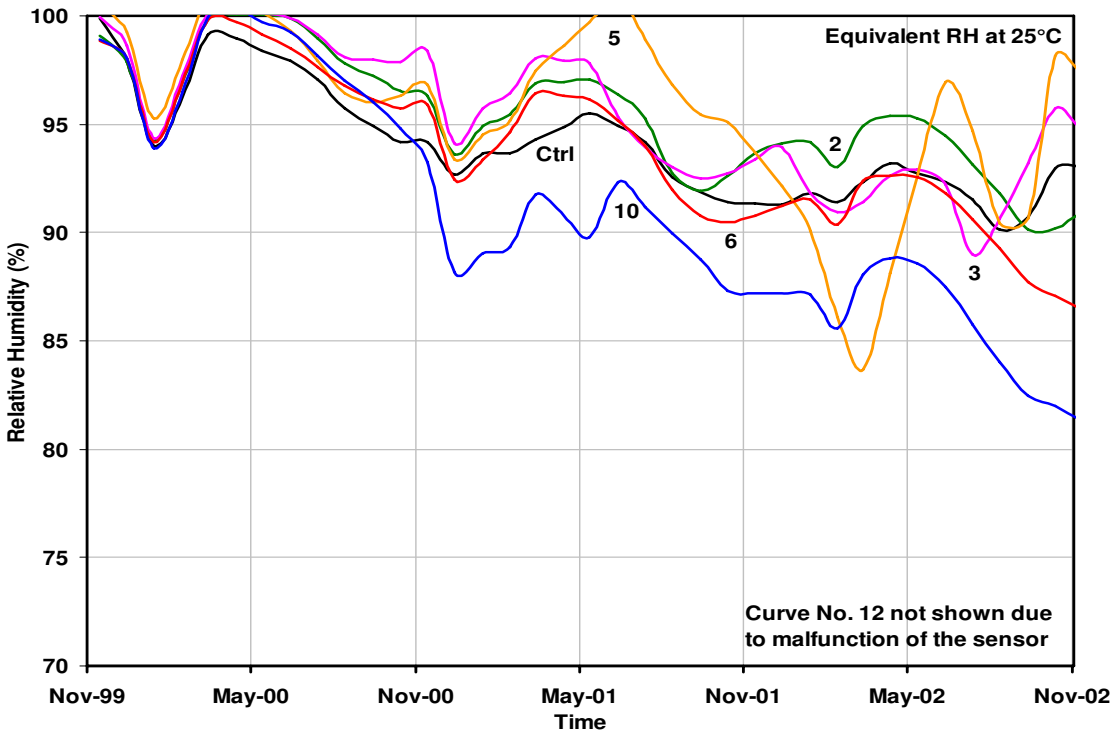

Fig. 6 – Monthly average relative humidity in concrete substrates

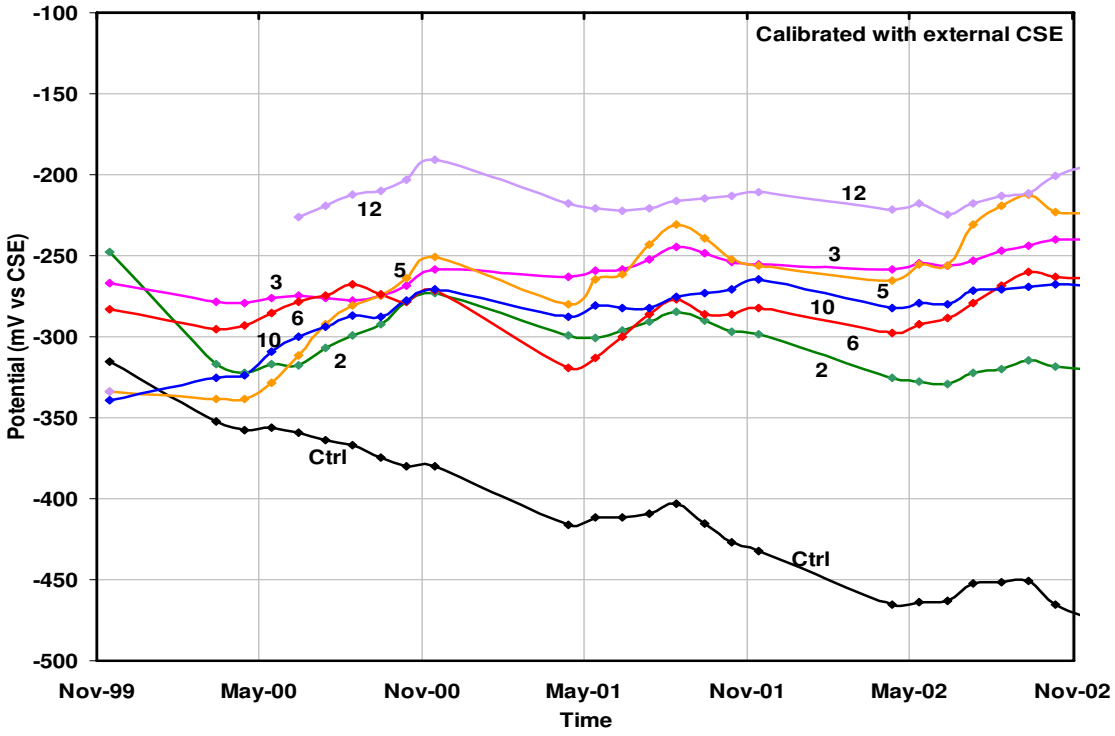

Fig. 7 – Monthly average corrosion potential in concrete patches (RE4)

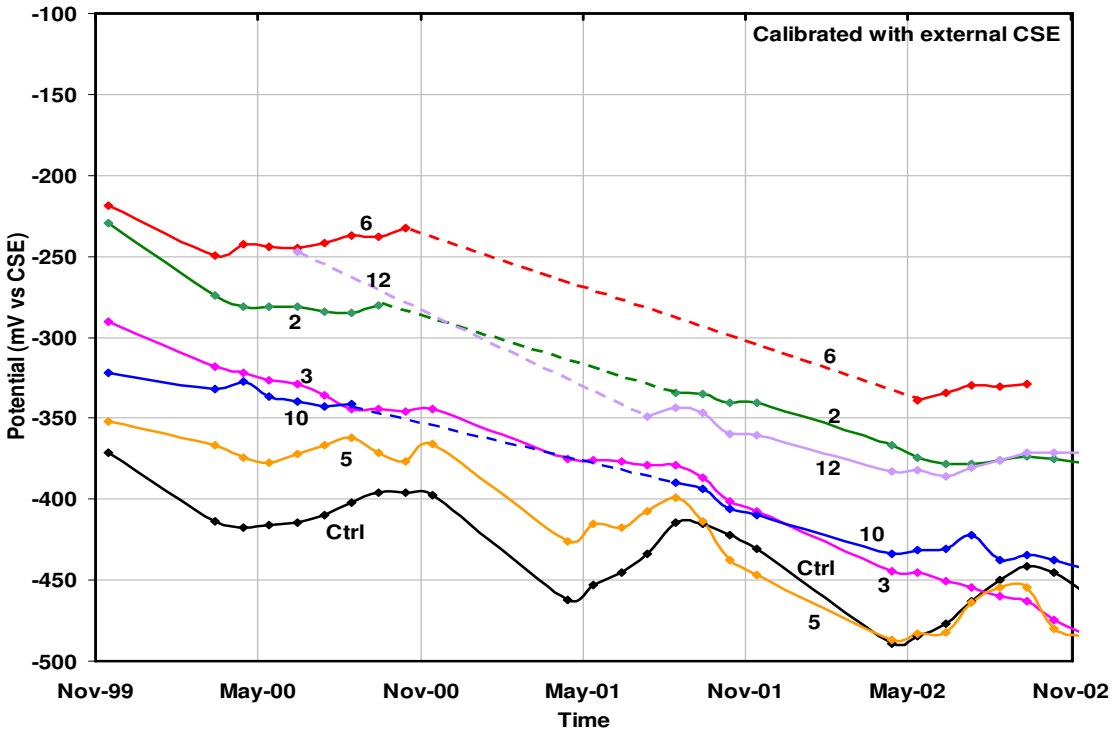

Fig. 8 – Monthly average corrosion potential in old concrete (RE1)

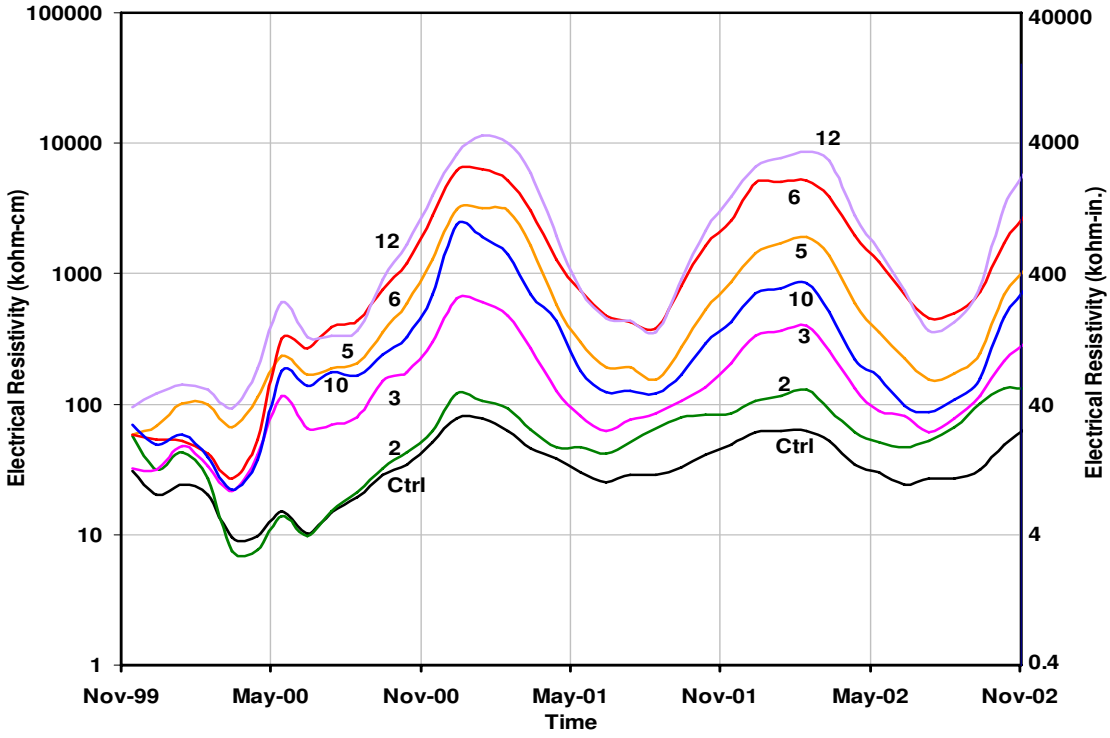

Fig. 9 – Monthly average electrical resistivity in concrete patches

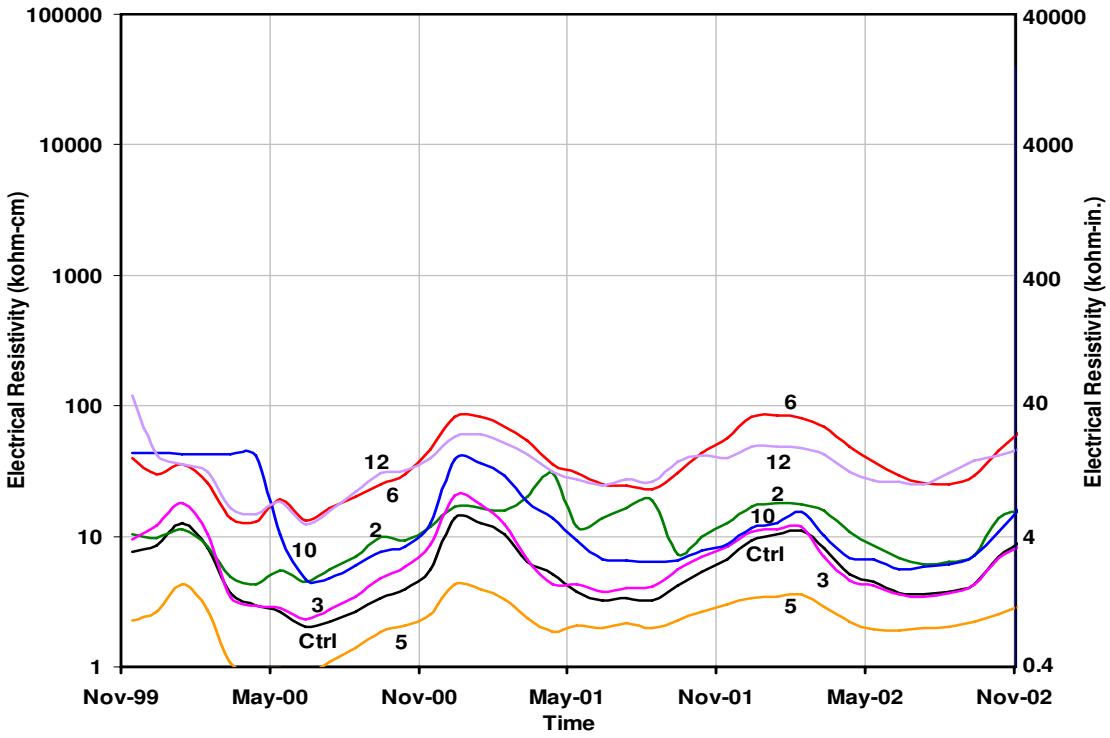

Fig. 10 – Monthly average electrical resistivity in old concrete

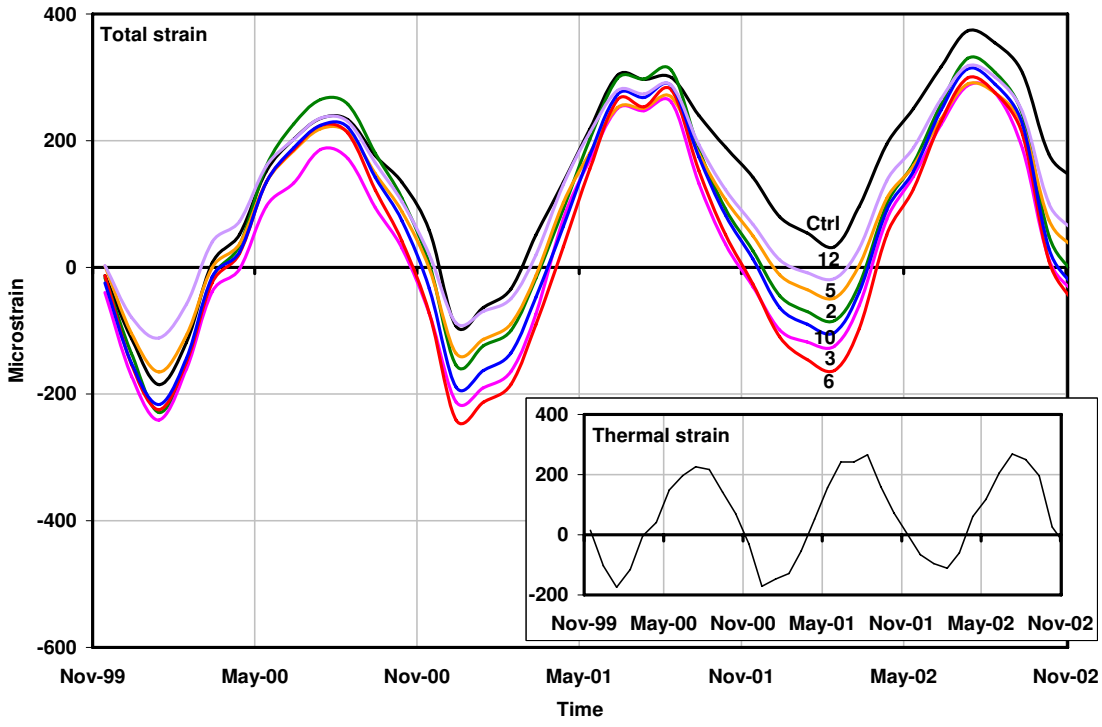

Fig. 11 – Monthly average transverse strain in concrete patches

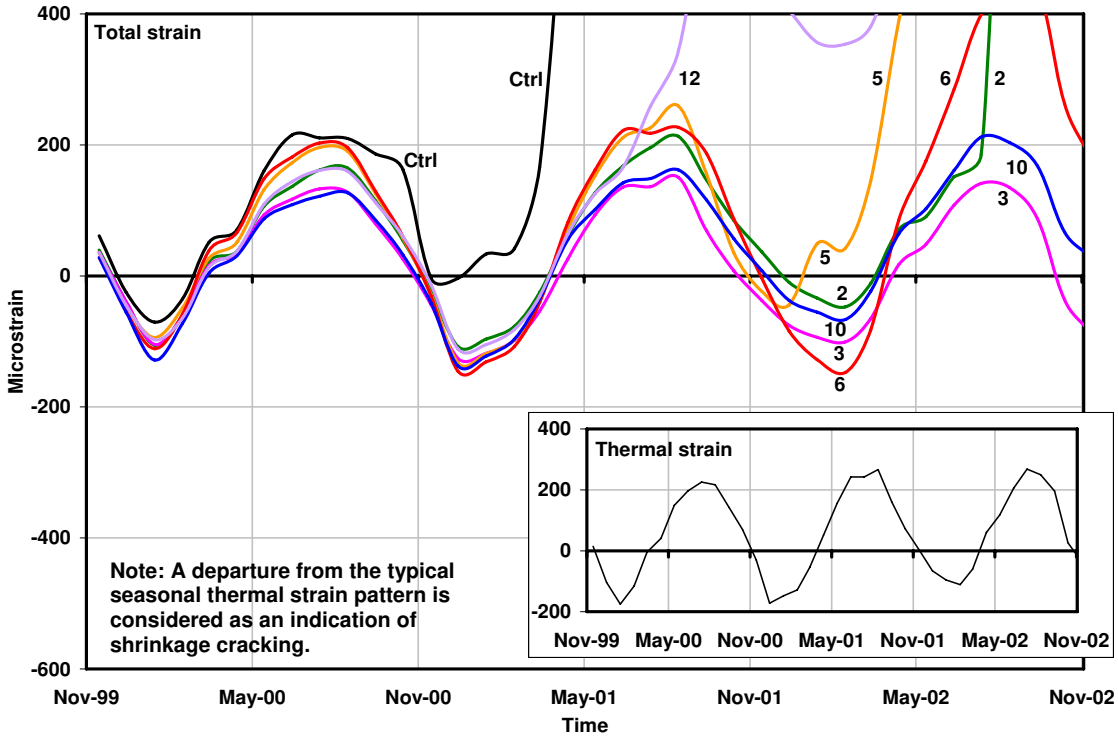

Fig. 12 – Monthly average longitudinal strain in concrete patches

Fig. 13 – Photograph of repaired Section 2 after four years (Oct. 2003)